

## 2-(Naphthalen-1-yl)thiophene as a New Motif for Porphyrinoids: Meso-Fused Carbaporphyrin

Jung-Ho Hong,<sup>†,‡</sup> Adil S. Aslam,<sup>†,‡</sup> Masatoshi Ishida,<sup>‡</sup> Shigeki Mori,<sup>§</sup> Hiroyuki Furuta,<sup>\*,‡</sup> and Dong-Gyu Cho<sup>\*,†</sup>

<sup>†</sup>Department of Chemistry, Functional Molecule Synthesis Laboratory, Inha University, Incheon 402-751, Republic of Korea

<sup>‡</sup>Department of Chemistry and Biochemistry, Graduate School of Engineering, and Education Center for Global Leaders in Molecular Systems for Devices, Kyushu University, Fukuoka 819-0395, Japan

<sup>§</sup>Integrated Center for Science, Ehime University, Matsuyama 790-8577, Japan

### S Supporting Information

**ABSTRACT:** The first synthesis of meso-fused carbaporphyrin via a premodification method was accomplished by substituting two pyrrole moieties and one meso-carbon with 2-(naphthalen-1-yl)thiophene. The obtained global  $\pi$ -conjugation pathway of the macrocycle noticeably disturbs the  $10\pi$  local aromaticity of naphthalene, and its aromatic nature was supported by NMR spectroscopy together with nucleus-independent chemical shift, anisotropy of the induced current density, and harmonic oscillator stabilization energy calculations. In addition, the meso-fused carbaporphyrin also allowed the formation of a square planar Pd<sup>II</sup> complex.

Porphyrin (1) is a natural pigment and aromatic macrocycle having four pyrroles that are fully conjugated with four meso-carbons. Its importance in living organisms cannot be disregarded (Figure 1).<sup>1</sup> Unlike natural porphyrins, new synthetic porphyrins (porphyrinoids) have been obtained either from direct synthetic precursors of the target molecule (premodifications) or from postmodifications of known porphyrins. These porphyrinoids have drawn considerable interest due to their different  $\pi$ -conjugation pathways from those of natural porphyrins, a variable degree of aromaticity, and their own unique metal coordination chemistry.<sup>2</sup> To obtain new porphyrinoids, premodification methods have been attempted by replacing the pyrrole moieties with new building blocks rather than simple thiophenes or furans (porphyrin (1) vs carbaporphyrin (2)). These synthetic approaches have been very challenging, and their rich chemistry has been proven in the field of synthetic porphyrinoid chemistry. Listed examples include *o*-(or *p*)-benzporphyrins,<sup>3</sup> naphthiporphyrins,<sup>4</sup> oxybenzporphyrins,<sup>5</sup> dithiaethyneporphyrin,<sup>6</sup> azuliporphyrins,<sup>7</sup> ferrocenothiaporphyrin,<sup>8</sup> N-confused porphyrins,<sup>9</sup> and neo-confused porphyrins.<sup>10</sup> On the other hand, many new porphyrinoids have also been synthesized by postmodification methods through common or known porphyrin intermediates. Consequently, these postmodifications potentially need new types of porphyrinoids that are formed via premodifications. Both synthetic approaches have their own merits. Thus, meso-fused porphyrins (4)<sup>11–14</sup> have been successfully accomplished from porphyrin intermediates such as meso-haloporphyrins,<sup>12</sup>

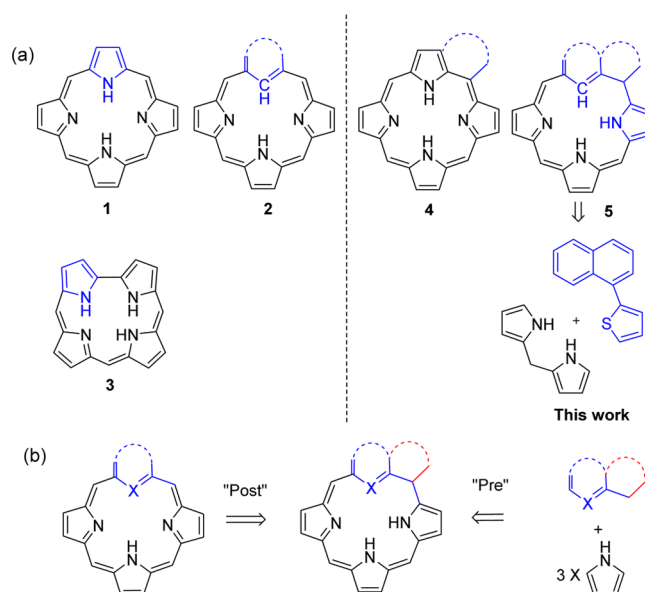


**Figure 1.** (a) Simplified structures of porphyrin (1), carbaporphyrin (2), corrole (3), meso-fused porphyrin (4), and conceptual drawings of the meso-fused carbaporphyrin (5) and its synthetic method reported herein. (b) Two different synthetic approaches (pre- vs post-modification).

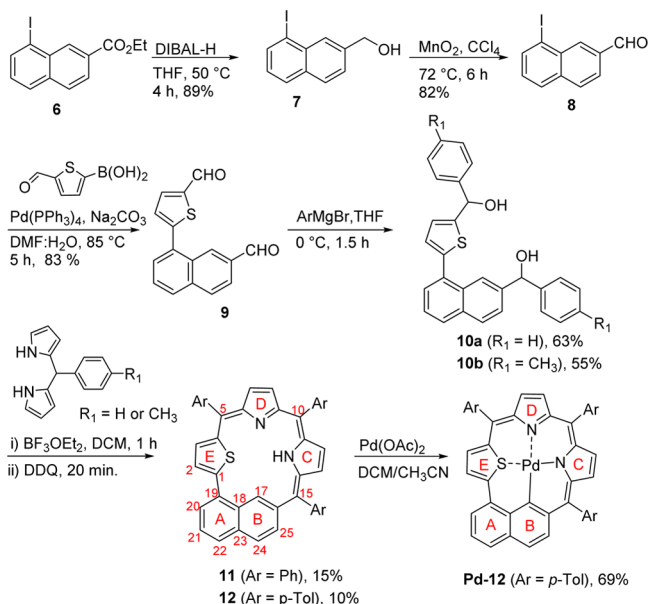
meso-unsubstituted  $\beta$ -haloporphyrins,<sup>13</sup> and zinc(II) 2,3,12,13-tetrabromo-tetraphenylporphyrin<sup>14</sup> via postmodification techniques. Structurally, meso-fused porphyrinoids are similar to corroles (3), contracted porphyrinoids formed by removing one of the meso-carbons of porphyrin. To date, to the best of our knowledge, meso-fused porphyrins have been rarely synthesized via a premodification method.<sup>15</sup> Herein, we report the first synthesis of a meso-fused carbaporphyrin (5)<sup>16</sup> via a premodification method using a new motif, 2-(naphthalen-1-yl)thiophene to replace two pyrroles and one meso-carbon, instead of one pyrrole. In this communication, its reduced aromaticity, unique electronic pathway that noticeably disturbs the  $10\pi$  local aromaticity of naphthalene, and metal coordination chemistry are discussed in connection with this new motif.

Received: January 29, 2016

Published: February 23, 2016

The synthesis of carbaporphyrin (**11**) was achieved by a modified [2 + 2] condensation of the naphthalene bis-carbinol derivative with a typical porphyrin precursor, dipyrromethane (Scheme 1).<sup>17</sup> A thiophene-substituted diformyl derivative (**9**)

### Scheme 1. Synthetic Scheme of Meso-Fused Carbaporphyrin and Its Pd<sup>II</sup> Complex



was used as the building block to prepare the carbaporphyrin because of the ease-of-handling of the product than the pyrrolic congener. First, ethyl 8-iodo-2-naphthoate (**6**) was reduced with diisobutylaluminum hydride (DIBAL) and subsequently reoxidized to the corresponding formyl derivative (**8**).<sup>18</sup> Then the Suzuki coupling of compound **8** with 5-formyl-2-thienylboronic acid afforded the corresponding dialdehyde **9** in 83% yield. Bis-carbinol (**10**) was obtained from compound **9** by a Grignard reaction. Then a Lewis-acid-catalyzed [2 + 2] reaction followed by the oxidation with 2,3-dichloro-5,6-dicyano-*p*-benzoquinone (DDQ) produced the target macrocycle **11** in 15% yield. Compound **11** was characterized by standard analytical techniques such as <sup>1</sup>H, <sup>13</sup>C, 2D-correlation spectroscopy (COSY), and nuclear Overhauser enhancement spectroscopy (NOESY) NMR spectroscopies and high-resolution mass analysis.

Suitable single-crystals of **11** were grown in CH<sub>2</sub>Cl<sub>2</sub>/*n*-hexane, and the structure was unambiguously elucidated by X-ray crystallographic analysis (Figure 2).<sup>19</sup> Each atom of naphthalene moiety is lying in a quasi-planar geometry with the range of deviations (0.003–1.057 Å) from the mean plane (defined with C5, C10, C15, and C19) (Figure S4 in the Supporting Information). Most β-carbons of pyrroles and thiophene atoms are located within 0.4–0.5 Å from the mean plane. In addition, larger dihedral angles were found around bonds such as C15–C16 (23.9°), C1–C19 (14.8°), and C4–C5 (10.7°) (Figure S5).

Supported by its relatively planar solid-state structure, the <sup>1</sup>H NMR spectrum of **11** is characteristic of aromatic porphyrins (Figure 3). The peripheral β-CHs and naphthalene-CHs are observed in the typical aromatic region (7.3–9.5 ppm). A combination of D<sub>2</sub>O exchange and 2D NMR experiments showed broad resonance peaks at 3.72 and 4.33 ppm that were assigned to the internal C<sup>17</sup>H and NH groups, respectively (Figure 3). The maximum difference between the chemical shifts

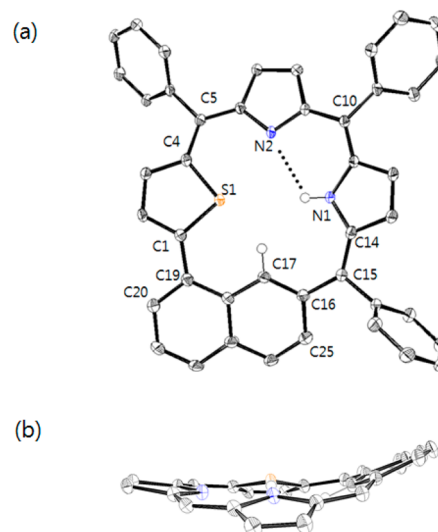


**Figure 2.** Molecular structure of **11**·CH<sub>2</sub>Cl<sub>2</sub>; (a) top view and (b) side view without meso-phenyl groups. Thermal ellipsoids are scaled to the 50% probability level. Most hydrogen atoms and residual solvent molecule are omitted for clarity. The potential hydrogen bonding is denoted by a dotted line.

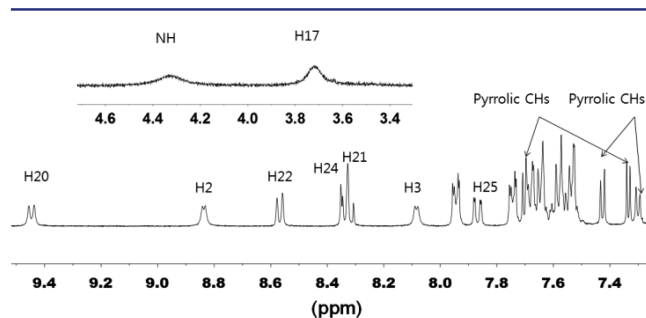


**Figure 3.** Partial <sup>1</sup>H NMR spectrum of **11** in CDCl<sub>3</sub> at 298 K. Inset shows the upfield region of the spectrum. Peak labels correspond to the systematic numbering shown in Scheme 1.

of the peripheral CH moieties and those of the interior CH or NH moieties is generally utilized as a benchmark for aromaticity. The values of  $\Delta\delta_{\text{CH-CH}} = 5.7$  (naphthalene) and  $\Delta\delta_{\text{CH-NH}} = 5.1$  ppm were comparable to those of the weakly aromatic *p*-benziporphyrin ( $\delta_{\text{CH-CH}} = 5.35$  ppm at 168 K),<sup>3b</sup> indicating the presence of a weak diatropic ring current in **11**. Moreover, the whole local aromaticity of naphthalene is noticeably disturbed by the global  $\pi$ -conjugation pathway of **11** due to its designed coplanar geometry. Thus, this disturbance is not clearly observed in 1,4-naphthiporphyrin.<sup>4b</sup> For example,  $\Delta\delta_{\text{CH-CH}}$  (naphthalene) is less than 0.9 ppm for 1,4-naphthiporphyrin, while a larger value ( $\Delta\delta_{\text{CH-CH}} = 5.7$ ) is observed on the naphthalene part of **11** at 298 K. The above results indicate that meso-fused carbaporphyrin is the very first aromatic macrocycle that noticeably disturbs the whole local aromaticity of aromatic molecules larger than  $6\pi$ .

The UV–visible absorption spectrum of **11** in CH<sub>2</sub>Cl<sub>2</sub> shows a characteristic intense Soret band at 429 nm ( $\epsilon = 6.02 \times 10^4 \text{ M}^{-1} \text{ cm}^{-1}$ ) accompanied by broad Q-like bands at 642 nm (Figure 4). These spectroscopic features of **11** likely resemble an aromatic porphyrin with an 18 $\pi$  electron circuit. The freebase **11** also exhibits a weak fluorescence emission at  $\lambda_{\text{max}} = 685$  nm, similarly indicating the aromatic character (Figure S3).

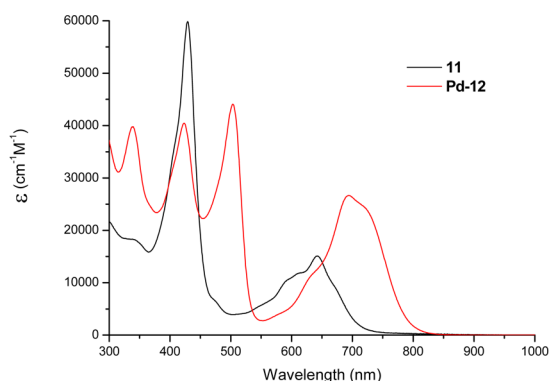


**Figure 4.** UV-vis absorption spectra of **11** and Pd-**12** recorded in  $\text{CH}_2\text{Cl}_2$ .

To investigate the electronic structure of **11**, density functional theory calculations were carried out (Figure S11). The optimized structure obtained by B3LYP/6-31G(d,p)-level calculations showed a similar geometric structure to that of the crystal structure. The reduced symmetric structure of **11** gave rise to the disordered four frontier orbitals of porphyrins with a broken degeneracy of HOMO and LUMO pairs (Figure S11). This was attributed to the reduced aromatic nature. By using the anisotropy of the induced current density (AICD) plot, the three-dimensional delocalized electron densities can be visualized with a vector field obtained by the current induced by an external magnetic field at each point in space.<sup>20</sup> As a result, the well-delocalized macrocyclic densities are represented in the structure of **11**, and the clockwise ring current was thus interpreted as its aromaticity (Figure S10). The weak aromatic nature of **11** was further supported by moderately negative nucleus-independent chemical shift (NICS) values (i.e.,  $\text{NICS}(0) = -5.3$  ppm) obtained at the central point of  $\pi$ -conjugated pathways in **11** (Figure S8). Importantly, two NICS(0) values at the center of the naphthalene ring (i.e., A and B) were determined to be  $-14.0$  and  $-6.3$  ppm, respectively, which are different from that of the original naphthalene ( $-8.6$  ppm, B3LYP/6-31G(d,p)) as shown in Figure S9. This also indicates the canonical conjugation circuit across the boundary of the local naphthalene subunit. To gain further insight into the canonical structures of **11** with either  $18\pi$  or  $22\pi$ -electron conjugation pathways, harmonic oscillator stabilization energy (HOSE) calculations were conducted based on the optimized structure obtained from the X-ray structure (Figure 5 and Table

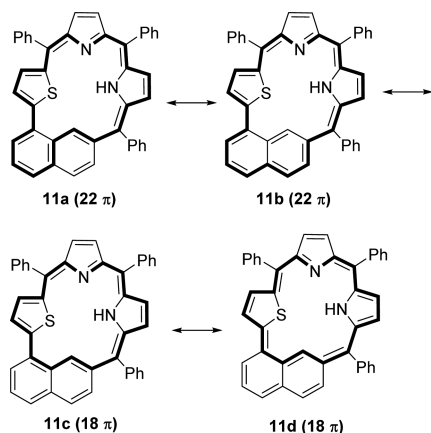


**Figure 5.** Possible canonical structures of **11**.

S3). These indices allowed the estimation of the contributions of particular canonical structures in  $\pi$ -electron systems. The  $22\pi$ -electron conjugated contributor **11a** probably best described the structure of **11** with a higher rate of 31.9%, while the rest of the structures **11b–d** had a rate of 25.6%, 28.6%, and 14.0%, respectively. Therefore, it should be noted that the  $22\pi$ -conjugative pathway in **11** is most likely; however, further structural studies may be necessary in the future.

The central cavity of carbaporphyrin **11** offers a dianionic coordination environment for metal ions with an “NNCS” mixed donor upon the activation of the interior C–H bond. A palladium(II) ion often affords a diamagnetic square-planar complex with regular porphyrins.<sup>21</sup> In some cases, carbaporphyrins have shown unique metal-mediated skeletal transformations via metal–arene interactions.<sup>22</sup> Thus, the reaction of freebase **12** with palladium(II) acetate was conducted in  $\text{CH}_2\text{Cl}_2$  containing 10%  $\text{CH}_3\text{CN}$  (Scheme 1).<sup>23</sup> After the chromatographic purification of the product, the high-resolution mass spectrum of the product showed the parent ion peak at  $m/z$  750.1314 (calcd for  $\text{C}_{46}\text{H}_{32}\text{N}_2\text{PdS}$   $[\text{M}]^+$ : 750.1321), indicating the formation of a mononuclear complex, Pd-**12**. Consistent with the mass data, the  $^1\text{H}$  NMR spectrum of Pd-**12** in  $\text{CDCl}_3$  showed the absence of the inner NH and CH signals in the entire spectral region because of cyclopalladation (Figure S2). The pyrrolic  $\beta$ -CHs resonated at 7.96, 7.82, 7.68, and 7.62 ppm, and the thiophenyl  $\beta$ -CHs appeared at 8.41 and 8.00 ppm. This indicates that the Pd complexation afforded similar geometric species as that of the free base. The detailed structure of complex **12** was also successfully confirmed by single-crystal X-ray diffraction (Figures 6 and S6).<sup>19</sup> The  $\text{Pd}^{\text{II}}$  metal center is connected by the

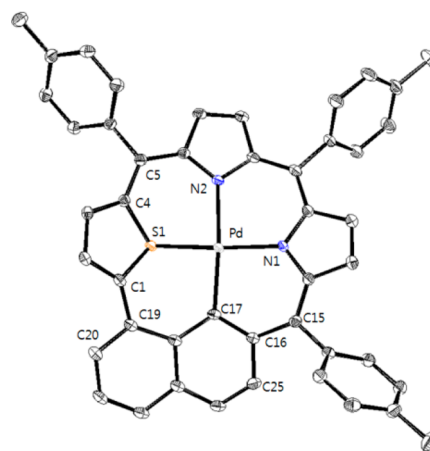


**Figure 6.** X-ray crystal structure of Pd-**12**·MeOH. Thermal ellipsoids are scaled to the 50% probability level. Most hydrogen atoms and disordered solvent molecules are omitted for clarity.

macrocyclic framework with bond lengths of 2.139 (Pd–N1), 2.025 (Pd–N2), 2.097 (Pd–C17), and 2.195 Å (Pd–S1). The shorter metal–carbon bond may have originated from the stronger  $\sigma$ -donor character of the naphthalene unit as observed in other carbaporphyrins.<sup>24</sup> The thiophene ring slightly tilted toward the mean plane with an angle of  $38.19^\circ$  (Figure S7). This distortion of the annulenic circuit reflects to the reduced diatropicity in Pd-**12**.

The electronic absorption spectrum of Pd-**12** shows split Soret-like bands at 423 and 503 nm and a Q-like band at 694 nm (Figure 4). Compared to the Q-band of **12**, the band red-shifted by 52 nm in Pd-**12** (Figure 4). This reflects the redox properties



of the porphyrin upon metal complexation. Therefore, the electrochemical properties of **11** and **Pd-12** in CH<sub>2</sub>Cl<sub>2</sub> containing 0.1 M *n*-Bu<sub>4</sub>NPF<sub>6</sub> as the electrolyte were investigated by cyclic voltammetry (Figure S13). In the voltammogram of **11**, two reversible oxidation waves were observed at  $E_{\text{ox}} = 0.28$  and 0.59 V (vs  $F_c/F_c^+$ ), and one reversible reduction potential was observed at  $E_{\text{red}} = -1.49$  V. The estimated highest occupied molecular orbital (HOMO)–lowest occupied molecular orbital (LUMO) energy gap of **11** was thus estimated to be 1.77 eV. The CV of **Pd-12** showed similar redox processes as **11** at 0.16, 0.84, and  $-1.52$  V. The Pd complex has a smaller HOMO–LUMO energy gap ( $E_{\text{gap}} = 1.68$  V) than that of **11**, consistent with the theoretical energy gap (Figures S11 and S12).

In summary, we report the first synthesis of meso-fused carbaporphyrin via a premodification method. The incorporated naphthalene moiety in **11** has a coplanar geometry, thus leading to significant disturbance in the whole local aromaticity of naphthalene when compared to other reported naphthoporphyrin compounds. Macrocycle **11** showed a distinct diatropic ring current in the NMR spectrum together with porphyrin-like photophysical features, even though these effects are weak. The electronic structure of **11** can be described as either an  $18\pi$  or a  $22\pi$  aromatic species as inferred from NICS, AICD, and HOSE calculations. Derivative **12** formed a diamagnetic square-planar Pd<sup>II</sup> complex. The unique  $\pi$ -conjugation pathway of meso-fused carbaporphyrin and its synthetic strategy to use 2-(naphthalen-1-yl)thiophene as an intermediate could be applied to understand other  $\pi$ -conjugation pathways and obtain new macrocycles.

## ■ ASSOCIATED CONTENT

### Supporting Information

The Supporting Information is available free of charge on the ACS Publications website at DOI: 10.1021/jacs.6b01063.

Experimental procedures, characterization data, theoretical calculations, and <sup>1</sup>H and <sup>13</sup>C NMR spectra for all new compounds (PDF)

X-ray data of **12** (CIF)

X-ray data of **Pd-12** (CIF)

## ■ AUTHOR INFORMATION

### Corresponding Authors

\*hfuruta@cstf.kyushu-u.ac.jp

\*dgcho@inha.ac.kr

### Author Contributions

<sup>†</sup>J.-H.H. and A.S.A. contributed equally.

### Notes

The authors declare no competing financial interest.

## ■ ACKNOWLEDGMENTS

This research was supported by the Basic Science Research Program through the National Research Foundation of Korea (NRF), funded by the Ministry of Education, Science, and Technology (Grant No. NRF-2013R1A1A2057508) and JSPS Grant-in-Aid for Scientific Research (25248039 and 26810024). D.-G.C. thanks the JSPS Invitational Fellowship (ID No. S151715).

## ■ REFERENCES

- (1) Vogel, E. *Pure Appl. Chem.* **1996**, *68*, 1355.
- (2) (a) Sessler, J. L.; Seidel, D. *Angew. Chem., Int. Ed.* **2003**, *42*, 5134. (b) Saito, S.; Osuka, A. *Angew. Chem., Int. Ed.* **2011**, *50*, 4342.

- (3) (a) Berlin, K.; Breitmaier, E. *Angew. Chem., Int. Ed. Engl.* **1994**, *33*, 1246. (b) Stepień, M.; Latos-Grażyński, L. *J. Am. Chem. Soc.* **2002**, *124*, 3838.

- (4) (a) Lash, T. D.; Young, A. M.; Rasmussen, J. M.; Ferrence, G. M. *J. Org. Chem.* **2011**, *76*, 5636. (b) Szyszko, B.; Latos-Grażyński, L. *Organometallics* **2011**, *30*, 4354.

- (5) Lash, T. D. *Angew. Chem., Int. Ed. Engl.* **1995**, *34*, 2533.

- (6) Berlicka, A.; Latos-Grażyński, L.; Lis, T. *Angew. Chem., Int. Ed.* **2005**, *44*, 5288.

- (7) Lash, T. D.; Chaney, S. T. *Angew. Chem., Int. Ed. Engl.* **1997**, *36*, 839.

- (8) Simkova, I.; Latos-Grażyński, L.; Stepień, M. *Angew. Chem., Int. Ed.* **2010**, *49*, 7665.

- (9) (a) Furuta, H.; Asano, T.; Ogawa, T. *J. Am. Chem. Soc.* **1994**, *116*, 767. (b) Maeda, H.; Osuka, A.; Furuta, H. *J. Am. Chem. Soc.* **2003**, *125*, 15690. (c) Toganoh, M.; Kimura, T.; Uno, H.; Furuta, H. *Angew. Chem., Int. Ed.* **2008**, *47*, 8913.

- (10) Lash, T. D.; Lammer, A. D.; Ferrence, G. M. *Angew. Chem., Int. Ed.* **2011**, *50*, 9718.

- (11) (a) Barloy, L.; Dolphin, D.; Dupre, D.; Wijesekera, T. P. *J. Org. Chem.* **1994**, *59*, 7976. (b) Richeter, S.; Jeandon, C.; Gisselbrecht, J.-P.; Ruppert, R.; Callot, H. J. *J. Am. Chem. Soc.* **2002**, *124*, 6168. (c) Fox, S.; Boyle, R. W. *Chem. Commun.* **2004**, 1322. (d) Davis, N. K. S.; Thompson, A. L.; Anderson, H. L. *J. Am. Chem. Soc.* **2011**, *133*, 30. (e) Pawlicki, M.; Hurej, K.; Kwiecinska, K.; Szterenber, L.; Latos-Grażyński, L. *Chem. Commun.* **2015**, *51*, 11362.

- (12) Sahoo, A. K.; Mori, S.; Shinokubo, H.; Osuka, A. *Angew. Chem., Int. Ed.* **2006**, *45*, 7972.

- (13) (a) Hata, H.; Shinokubo, H.; Osuka, A. *J. Am. Chem. Soc.* **2005**, *127*, 8264. (b) Fukui, N.; Yorimitsu, H.; Lim, J. M.; Kim, D.; Osuka, A. *Angew. Chem., Int. Ed.* **2014**, *53*, 4395. (c) Fujimoto, K.; Yorimitsu, H.; Osuka, A. *Org. Lett.* **2014**, *16*, 972. (d) Fukui, N.; Yorimitsu, H.; Osuka, A. *Angew. Chem., Int. Ed.* **2015**, *54*, 6311.

- (14) Ishizuka, T.; Saegusa, Y.; Shiota, Y.; Ohtake, K.; Yoshizawa, K.; Kojima, T. *Chem. Commun.* **2013**, *49*, 5939.

- (15) The  $\beta$ -substituted metal free version of indenoporphyrins<sup>11a</sup> was resynthesized via direct synthetic precursors (premodification). There is another meso-fused porphyrinoid synthesized from carbazole and pyridine precursors. See: (a) Lash, T. D.; Smith, B. E.; Melquist, M. J.; Godfrey, B. A. *J. Org. Chem.* **2011**, *76*, 5335. (b) Arnold, L.; Norouzi-Arasi, H.; Wagner, M.; Enkelmann, V.; Mullen, K. *Chem. Commun.* **2011**, *47*, 970.

- (16) Examples are all meso-fused N-confused porphyrins synthesized from a N-confused porphyrin. See: (a) Chmielewski, P. J.; Maciołek, J.; Szterenber, L. *Eur. J. Org. Chem.* **2009**, *2009*, 3930. (b) Liu, B.; Li, X.; Maciołek, J.; Stepień, M.; Chmielewski, P. J. *J. Org. Chem.* **2014**, *79*, 3129.

- (17) Gryko, D.; Lindsey, J. S. *J. Org. Chem.* **2000**, *65*, 2249.

- (18) Ethyl 8-iodo-2-naphthoate was synthesized from ethyl 8-amino-2-naphthoate.

- (19) CCDC 1438469 and CCDC 1438470 (**11** and **Pd-12**, respectively) contain the supplementary crystallographic data for this paper. These data can be obtained free of charge from the Cambridge Crystallographic Data Centre via [www.ccdc.cam.ac.uk/data\\_request/cif](http://www.ccdc.cam.ac.uk/data_request/cif).

- (20) Geuenich, D.; Hess, K.; Köhler, F.; Herges, R. *Chem. Rev.* **2005**, *105*, 3758.

- (21) Fleischer, E. B.; Miller, C. K.; Webb, L. E. *J. Am. Chem. Soc.* **1964**, *86*, 2342.

- (22) Szyszko, B.; Latos-Grażyński, L. *Chem. Soc. Rev.* **2015**, *44*, 3588.

- (23) Carbaporphyrin **12** was prepared to assign chemical shifts of **11** and improve the solubility of **Pd-11** in organic solvents.

- (24) Furuta, H.; Maeda, H.; Osuka, A.; Yasutake, M.; Shinmyozu, T.; Ishikawa, Y. *Chem. Commun.* **2000**, 1143.

## ■ NOTE ADDED AFTER ASAP PUBLICATION

TOC graphic was corrected on March 4, 2016.